Journal of Mechanical Engineering and Sciences
ISSN (Print): 2289-4659; e-ISSN: 2231-8380
Volume 13, Issue 4, pp. 5848-5861, December 2019

DOI: https://doi.org/10.15282/jmes.13.4.2019.10.0466

Sliding wear characteristics of FDM-processed polylactic-acid in bovine blood serum

B. Arifvianto*, A. T. Putra, B. T. Prayoga, R. Dharmastiti, U. A. Salim, M. Mahardika, Suyitno

Centre for Innovation of Medical Equipments and Devices (CIMEDs)
Department of Mechanical and Industrial Engineering, Faculty of Engineering,
Universitas Gadjah Mada
Jl. Grafika 2 Yogyakarta 55281, Indonesia
*E-mail: b.arifvianto@gmail.com; budi.arif@ugm.ac.id

ABSTRACT

Fused deposition modelling (FDM) has so far been recognized for its reliability and simplicity for manufacturing of geometrically-complex polymeric materials with 3D printing technique. Recently, the studies concerning the properties of materials fabricated by using the FDM have been growing, including those related to their wear resistance which is considered of critical when a 3D-printed material must work sliding over the surface of another material during its application. Up to now, however, the influence of several FDM-printing parameters, including the raster orientations, on the wear resistance of the printed polymeric materials have not yet been fully understood. In this research, the influence of raster orientations on the wear resistance of FDM-processed polylactic-acid (PLA) materials in bovine blood serum were determined. A reciprocating pin-on-plate tribometer was used to evaluate wear resistance of a cylindrical PLA pin that slid over the surface of a commercially-pure titanium (Ti) plate. The results showed that the FDM-printed PLA pins with unidirectional raster orientations had higher wear factors (*WF*), i.e., ~1.5×10^{-4} mm N^{-1} m^{-1} than those with crossed raster orientations, i.e., ~0.8×10^{-4} mm N^{-1} m^{-1}. Meanwhile, the *WF* values of Ti surface that slid against PLA pin with crossed raster orientations, i.e., ~0.09×10^{-4} mm N^{-1} m^{-1}, were also significantly lower than those sliding with the pin having unidirectional raster orientation, i.e., $0.34 – 0.41 \times 10^{-4}$ mm N^{-1} m^{-1}. The result of analysis of the worn surface morphologies shows the indications of surface abrasion, fatigue and polymer film transfer as the possible wear mechanisms of both the FDM-processed PLA pin and its Ti countersurface material. On the basis of all the findings in this research, it can be concluded that the crossed raster orientation is preferable to be used as one of the parameters in printing of the wear resistant PLA rather than the unidirectional raster orientation.

Keywords**:** wear; fused deposition modelling; raster orientation; polylactic-acid; titanium

INTRODUCTION

Recently, additive manufacturing has become a promising technique for the fabrication of geometrically-complex parts [1-4] and patient-specific biomedical implants [5, 6]. Among this technique, fused deposition modelling (FDM) has been recognized since the last decade and gained enormous attention from researchers worldwide, owing to its simplicity and reliability for building-up such complex-shape parts from polymeric materials [7]. In this technique, a molten filament of a polymeric material is extruded, deposited and then allowed to solidify to form multiple layers that build up a solid 3-dimensional (3D) material [1, 8]. So far, the FDM-printed product had been widely used for modelling and rapid prototyping [7]. However, the interest towards the use of functional polymeric products fabricated by using FDM has been growing, as indicated by the increasing number of studies which were carried out to investigate some important properties of such the additively manufactured material.

Wear resistance is considered as the important property of a functional material which must work in sliding over the surface of another material during its application. However, only a limited number of studies has so far been dedicated to reveal the wear characteristics of FDM-processed polymeric materials. In earlier studies [8, 9], the wear resistance of an FDM-printed material is governed by the inter-layer and/or inter-raster strength of the deposited material that built-up the printed product. In this case, the inter-layer and/or inter-raster bonding region was obviously of the weak region where the wear failure of the FDM-printed materials was often initiated [8]. Furthermore, the FDM processing parameters for printing acrylonitrile butadiene styrene (ABS) part, such as part build orientation, layer thickness and raster angle, all determined the wear behaviours of this material once tested in pin-on-disc tribometer at dry condition [8-10]. Also reported previously, the presence of the debris flanked at the sliding interface between the tested materials contributed to increase the wear through adhesion, abrasion and crack development over the sliding surface of the FDM-printed material [9]. To the more relevant application for biomedical implants, however, such a dry tribological test could not appropriately mimic the wear mechanisms that occurred in the knee or hip joints.

So far, tribological studies of an FDM-processed polymeric part in a lubricated sliding system had only been reported recently by Borges et al. [11]. In their work, an FDM-printed polycarbonate-urethane (PCU) and its blend with ultra-high molecular weight polyethylene (UHMWPE) were tested in a pin-on-disc tribometer, with bovine serum as the lubricant. The result of this study showed the importance of inherent pores generated by the FDM to reduce the friction coefficient of the printed material after certain duration of testing. In this case, the pores at the surface and interior of FDM-printed PCU and its blends were capable of absorbing bovine serum and thus providing sufficient lubrication to the sliding surfaces of both materials during the test [10]. Nevertheless, the limited number of works has called further researches in this particular topic. For instance, the influence of raster orientations on the wear resistance of a printed in the FDM-processed polymeric material in a lubricated system has not yet been fully understood, causing difficulty in selecting the appropriate parameter of raster orientation that could be used to improve wear resistance of the printed material.

In this research, the wear characteristics of polylactic-acid (PLA) material fabricated by using FDM were studied with blood bovine serum as the lubricant. Two raster orientations, i.e., unidirectional and crossed orientations, were printed to realize PLA pins and four sliding configurations were then performed in the experiment. The tribological test was carried out in a reciprocating pin-on-plate tribometer, aiming to determine wear factors of the FDM-printed PLA pin and its titanium (Ti) countersurface material. Characterizations of the worn surfaces of both the PLA pin and the Ti plate were then conducted to aid in establishing possible wear mechanisms that occurred during the sliding test.

MATERIALS AND METHODS

Materials Preparation

In this research, a cylindrical PLA material printed by using FDM and a Grade 2 Ti sheet were prepared as the pin and the plate for a pin-on-plate sliding test, respectively. The PLA pin was printed with 8.1 mm and 20 mm in diameter and height, respectively, according to the standard dimensions for pin-on-disc wear testing for biomaterials used for total joint replacement [12]. Two groups of PLA pin were prepared with unidirectional and crossed raster configurations, such as illustrated schematically in Figure 1. Figure 1(a) shows the internal structure of PLA pin printed with unidirectional raster configuration, in which multiple layers of rasters were all printed in single direction. Meanwhile, the PLA pin printed with crossed raster configuration was prepared firstly by depositing a layer of unidirectional raster. Another layer having unidirectional raster configuration was then deposited, directed perpendicular to the deposited rasters of the preceding layer. Such a material deposition pattern was repeated until a cylindrical PLA pin with aforementioned height was realized, such as shown in Fig. 1(b). Table 1 presents a set of technical parameters that were used in the printing of PLA pin by using the FDM.

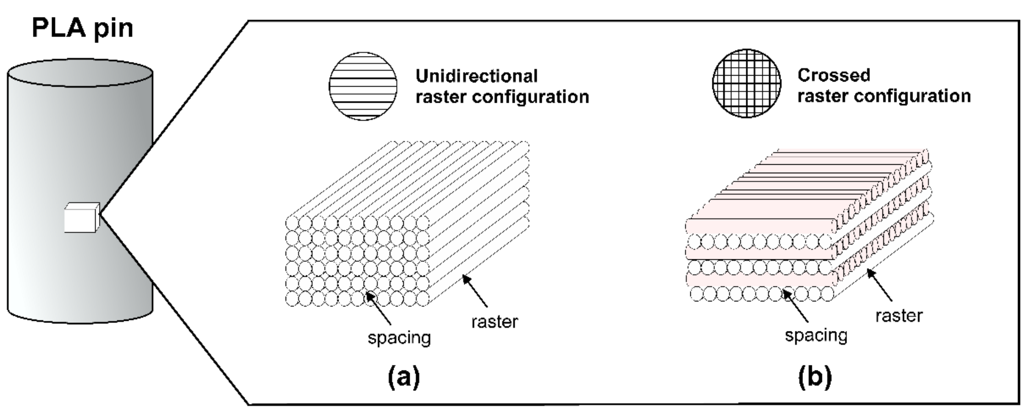

Figure 1. Raster configurations designed in the PLA pin: (a) unidirectional and (b) crossed raster configurations.

Table 1. FDM-processing parameters used for the preparation of PLA pin.

Parameters	Quantity
Filament diameter	1.75 mm
Printing temperature	195 °C
Deposition speed	50 mm s^{-1}
Perimeter thickness	0.8 mm
% infill	100%
Layer thickness	0.2 mm

To indicate the presence of pores in the interior of the FDM-processed PLA pin, the porosity (p) of this material was determined based on its relative density, as can be calculated by using Equation. (1):

$$p = \left(1 - \frac{\rho}{\rho_s}\right) \times 100\% \quad (1)$$

where ρ and ρ_s are the actual and theoretical density of the PLA pin, respectively. In this case, ρ_s = 1.21 g cm^{-3} was established as the theoretical density of the PLA material. As a countersurface material for the PLA pin during the sliding test, a casted and polished Ti plate was prepared with a dimension of 55 mm × 18 mm × 3 mm.

Tribological Test

In this research, a series of sliding tests was carried out with four pin-on-plate sliding configurations such as seen in Figure 2. The U1 and U2 configurations utilized PLA pins with unidirectional raster orientation, but being positioned so that their rasters were parallel (Figure 2(a)) and perpendicular (Figure 2(b)) to the sliding direction, respectively. Meanwhile, the PLA pins with crossed raster orientation were used in the sliding test with C1 and C2 configurations. Both were also positioned so that the relative orientations of their crossed raster to the pin sliding direction over the Ti plate surface apparently formed "+" and "×" configurations such as seen in Figures 2(c) and (d), respectively.

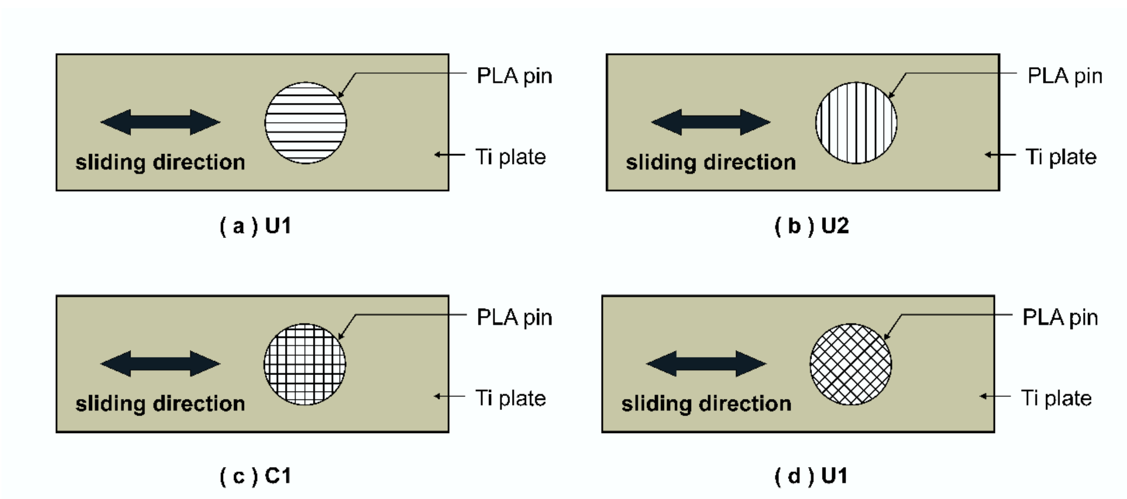

Figure 2. Sliding test configurations used in this research.

The sliding test of the PLA pin over the surface of the Ti plate was performed at room temperature and with a normal load of 120 N which could deliver a contact stress of 1.82 MPa over the sliding interface between the pin and the plate. Such obtained contact stress was lying within the acceptable value range that represent the in vivo clinical condition for total joint replacement (TJR), i.e., 1.1 – 3.5 MPa [12]. Similarly, a sliding speed of 50 mm s^{-1} was also preferred considering the acceptable speed range for the *in vivo* clinical condition of TJR [12]. During the sliding test, all the contact surfaces of the cylindrical PLA pin and the Ti plate were kept immersed in lubricant. Bovine blood serum with protein content of 67.7 g/L was selected as the lubricant in this research, considering its wide applications for tribological testing of biomedical materials [12, 13]. Detailed information related to the preparation of the bovine blood serum and the sliding test experiment conducted in this research were described in a previous study [14].

The wear characteristics of both the PLA pin and the Ti plate were determined from their weight losses, which could be calculated by using Equation. (2):

$$w_L(\%) = 1 - \frac{w_t}{w_0} \times 100\% \quad (2)$$

where w_0 and w_t are the initial weight and the weight of material after certain distance had been reached, respectively. In addition, wear factors (*WF*) of both the PLA pin and the Ti plate were determined by using Equation. (3) to obtain intrinsic wear resistance of these materials:

$$WF = \frac{V_w}{N \cdot s} \quad (3)$$

where V_w is the wear volume, N is the normal load applied to the cylindrical pin, and s is the sliding distance travelled by the pin over the plate surface.

Surface Characterizations

Characterizations of both the initial and worn surfaces of the PLA pin and the Ti plate were carried out by using a stylus profilometer (Surfcom 120A, Advanced Metrology System, UK) and an electron microscope (JSM-6510LV, JEOL Ltd., Japan) to determine their roughness and morphologies, respectively. Also, elemental compositions of the sliding surfaces of both these materials were determined by using energy-dispersive X-ray spectroscopy (EDS), prior to and after the sliding test.

Statistical Analysis

In this research, a statistical analysis was conducted by using one-way ANOVA with p = 0.05 and performed in Microsoft Excel 2016 to aid in determining the influence of raster orientations printed in the PLA pins on their wear factors obtained.

RESULTS AND DISCUSSION

In this research, the sliding wear characteristics of a pair of FDM-printed PLA pin and polished Ti plate were studied by using a pin-on-plate tribometer with bovine blood serum as the lubricant. Despite its versatility for the fabrication of customized and geometrically-complex shape materials and biomedical implants [1, 6], the FDM technology still possessed several limitations. For instance, a porous-free 3D solid material could hardly be produced with this technique, which in the end could compromize the mechanical and tribological properties of the printed materials [8, 16]. In this study, the presence of porous structure in the interior of all the FDM-processed PLA pins was confirmed from their calculated porosities, i.e., 5.5% and 4.8% for the pins with unidirectional and crossed raster orientations, respectively. As reported earlier, pores with total porosity of 6.3 – 13.6% were present at the interior of the FDM-processed polyurethane and its blend with polyethylene [10]. Pores generated at the interior and the surface of the FDM-processed materials corresponded to the spacing between the two adjacent rasters in the printed material [9], as indicated schematically in Figure 1(a).

To indicate the spacing between the adjacent rasters over the sliding surface of the FDM-processed pin, the sliding surface morphologies of all the PLA pins prior to the tribological test were examined and the results were presented in Figures 3(a) and (b). As seen in these figures, all the spacings at the sliding surface of the PLA pin could be easily recognized, as indicated by linear white defects shown in the micrographs. Interestingly, all the spacings at the PLA pin prepared with crossed raster configuration were less obvious than those on the pin surface printed with unidirectional raster configuration. The presence of spacings increased the roughness of the PLA pin surface, as confirmed in the earlier work [8]. As shown in Table 2, the measured sliding surface roughness of the PLA pin, in the form of R_a value, was 3.44 ± 0.07 μm and 1.97 ± 0.01 μm for the pin with unidirectional and crossed raster configurations, respectively. Meanwhile, a flat, smooth and shiny Ti surface with R_a = 0.1 ± 0.01 μm was prepared as the countersurface for the FDM-processed PLA pin during the sliding test, such as shown in Figure 3(c).

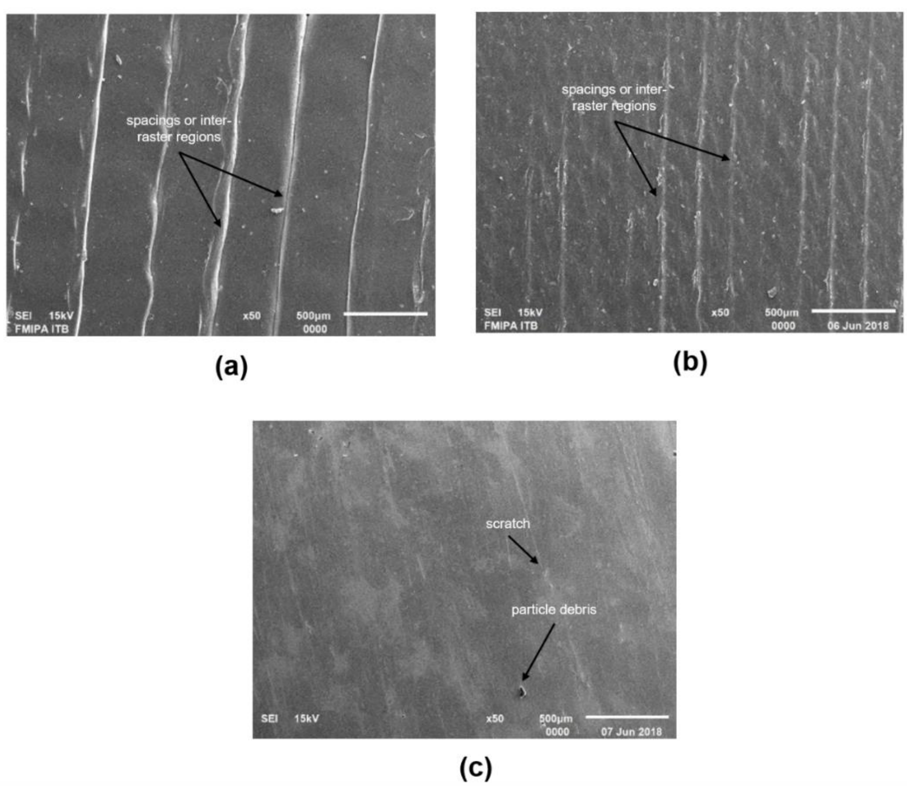

Figure 3. Initial morphologies of the sliding surface of (a) PLA pin with unidirectional raster orientation, (b) PLA pin with crossed raster orientation, and (c) Ti plate.

As can be seen in Figures 4(a) and (b), the weight losses (w_L) of both the FDM-printed PLA pin and Ti plate generally increased with the sliding distance travelled by both the materials during the experiment. More importantly, the wear resistance of the sliding materials could be seen from the calculated wear factor (*WF*) in Figure 5, which were determined based on the weight losses of all these materials after sliding for a distance up to 4×10^3 m. Based on the results of analysis by using one-way ANOVA, it is revealed that there was no significant difference on the *WF* values between the PLA pin printed with U1 and U2 configurations. Similarly, the *WF* values of the PLA pin printed with C1 was not statistically different with that printed with C2 configuration. However, the wear resistance of the PLA pin with unidirectional raster configuration was statistically lower than that of the pin printed with crossed raster configuration, as indicated from the higher *WF* values of the former groups of materials.

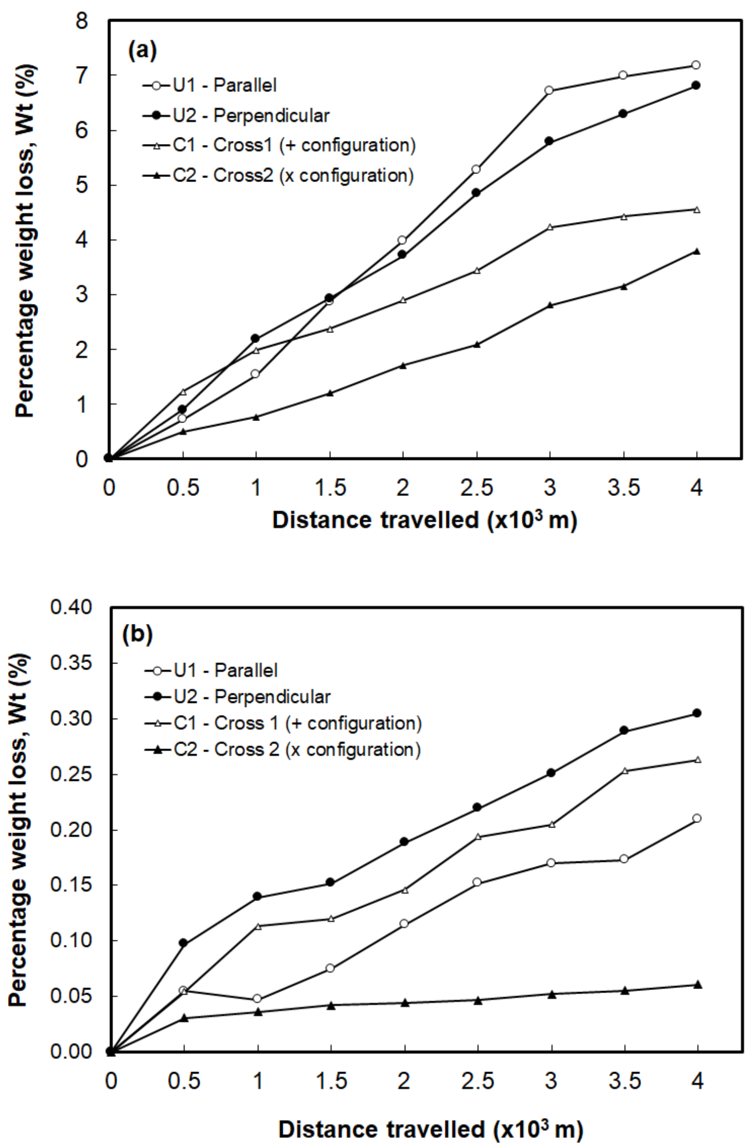

Figure 4. Weight losses of (a) PLA pin and (b) Ti plate during the sliding test.

Since the porosity of the PLA pins with the U1 and U2 raster orientations was slightly higher than those with C1 and C2, this study confirmed that the porosity generated by the FDM process was one of deteriorating factors for wear resistance of the printed material. In this case, the higher porosity would decrease material integrity against the applied load and sliding motion during the test. In earlier studies, however, the presence of porous structure of the FDM-printed material would aid in retaining lubricant fluid during the sliding test [10]. As also noted earlier [10], the FDM-printed polymeric material with a higher surface roughness would be having higher wear rate compared with the smoother one. In Table 2, it is shown that the initial R_a value of the PLA pin printed with unidirectional raster orientation was higher than that with the crossed one. In connection to the results in Figures 4(a) and 5, it could then be confirmed that the increased roughness would lead to reduction of wear resistance of FDM-printed PLA pin. During the sliding, the rough but soft asperities of the PLA pin surface would be cut off by the smooth but hard surface of the Ti counter material during the sliding. As a result, surface smoothening occurred in the PLA pin, as indicated by the decreased R_a value of the PLA pin after the sliding test. In the case of PLA pins with unidirectional raster orientation, the presence of the more irregular asperities or bumps in such a rough surface might be easier for the smooth Ti surface to cut off rather than those having the more regularly-structured surface of printed PLA with crossed raster orientation. Based on these results, it can be noted that the higher wear loss of the printed PLA with unidirectional raster orientation was attributed by two factors, i.e., the higher porosity and the rougher sliding surface of this material compared with those printed with crossed raster configuration. Further studies are still needed to investigate the role of pores on the wear behavior of the FDM-printed part in lubricated system.

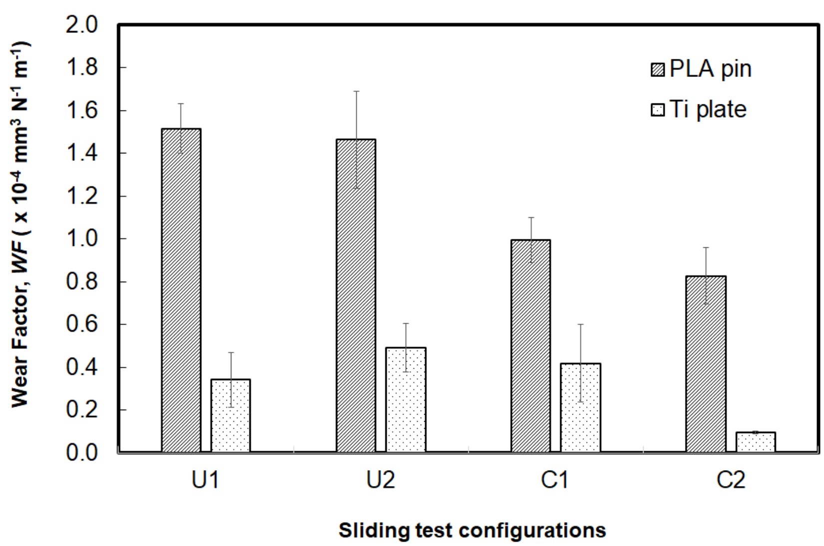

Figure 5. Wear factors of the PLA pin and the Ti plate.

Table 2. Sliding surface roughness of the PLA pin and the Ti plate.

Sliding test configurations	**PLA pin**		**Ti plate**	
	R_a, prior to sliding test (μm)	**R_a, after sliding test (μm)**	**R_a, prior to sliding test (μm)**	**R_a, after sliding test (μm)**
U1	3.44 ± 0.07	2.68 ± 0.08	0.10 ± 0.01	2.47 ± 0.26
U2	3.44 ± 0.07	2.41 ± 0.08	0.10 ± 0.01	2.39 ± 0.02
C1	1.97 ± 0.01	1.42 ± 0.08	0.10 ± 0.01	2.28 ± 0.09
C2	1.97 ± 0.01	0.56 ± 0.50	0.10 ± 0.01	0.99 ± 0.02

* R_a = arithmetic medium value

The calculated *WF* values of all the Ti countersuface material are shown in Figure 5. The result of statistical analysis by using one-way ANOVA however shows no significant difference among the *WF* values of the Ti plate after sliding against PLA pin with U1, U2 and C1 testing configurations. Meanwhile, the *WF* value of Ti plate that slid against PLA pin with C2 configuration was statistically lower than all the plates tested with the other raster configurations. On the basis of all the results obtained in Figures 4 and 5, therefore, the use C2 testing configuration was beneficial and could be preferred to reduce wear loss of both the FDM-printed PLA and its Ti countersurface compared with other testing configurations studied in this research.

To aid in establishing possible wear mechanisms of the FDM-printed PLA material, the sliding surface morphologies of all the pins after the tribological test are examined and the results are presented in Figure 6. Obviously, the micrographs in Figures 6(a) and (b) show the presence of acicular scars that were formed at the weak region of the interface between two adjacent rasters. As also demonstrated in these figures, the orientation of such acicular scars depended on the raster and the sliding test configurations. In this case, the wear scar of the PLA pin tested with U1 sliding configuration was stretched parallel to the direction of sliding and to the scratches that occurred over the pin surface (Figure 6(a)). Meanwhile, scars stretched perpendicular to the sliding direction was visible at the worn surface of PLA pin that was tested with U2 sliding configuration (Figure 6(b)), showing the opening of the spacing between two adjacent rasters. In contrast to the findings in Figures 6(a) and (b), all the worn surfaces of PLA pins with printed crossed raster orientation did not indicate the presence of such acicular scars, such as shown in Figures 6(c) and (d).

In earlier study, it is proposed that the wear mechanism of the FDM-printed ABS during a pin-on-disc sliding test corresponded to the presence of trapped debris particles in the spacing between two adjacent rasters over the sliding surface of the material [9]. As they were compressed by the contact pressure, such trapped particles would then cause deformation and initiate the other wear mechanisms, such as adhesive wear, fatigue wear and abrasion. Considering a smoother initial surface of the harder Ti plate, the wear debris particles could be generated from both the PLA pin and Ti plate surfaces during the sliding test. Once received contact stress, local strain hardening might occur at both the PLA surface asperities and its loose wear debris particles, from which they might be able to plough and produce rough Ti surface and generated another debris particle from this countersurface material. Together with the rough Ti surface, both the wear debris from the PLA pin and Ti plate would then contribute to the abrasion of the sliding surface of PLA pin.

Similar to the earlier work [9], the presence of wear scars in the form of pits and linear scratches shown in Figure 6(a) and (b) obviously confirmed the occurrence of fatigue and abrasive wear mechanisms, respectively, on the sliding surface of the printed PLA pins with unidirectional raster orientations. Meanwhile, only abrasive wear was evident to take place at the sliding surface of PLA pins with crossed raster orientations, such as seen in Figure 6(c) and (d). In all these micrographs, all the scratches were visible with orientations toward the sliding direction of the pin.

In addition to the analysis based on the worn surface morphologies, elemental compositions of the sliding surface of the PLA pin were characterized by using EDS. As seen in Figure 6(e), the EDS spectra showed the presence of carbon (C) and oxygen (O) as the main elements that existed over the surface of the PLA pin. More importantly, the result of the EDS analysis also showed the presence of Ti element over the worn surface of the PLA pin, although its quantity was negligible on the pin surfaces tested with C1 and C2 configurations. This implied that the worn PLA pin surface contained Ti debris particles which firmly attached and could not be removed even having been cleaned with the procedure carried out in this research.

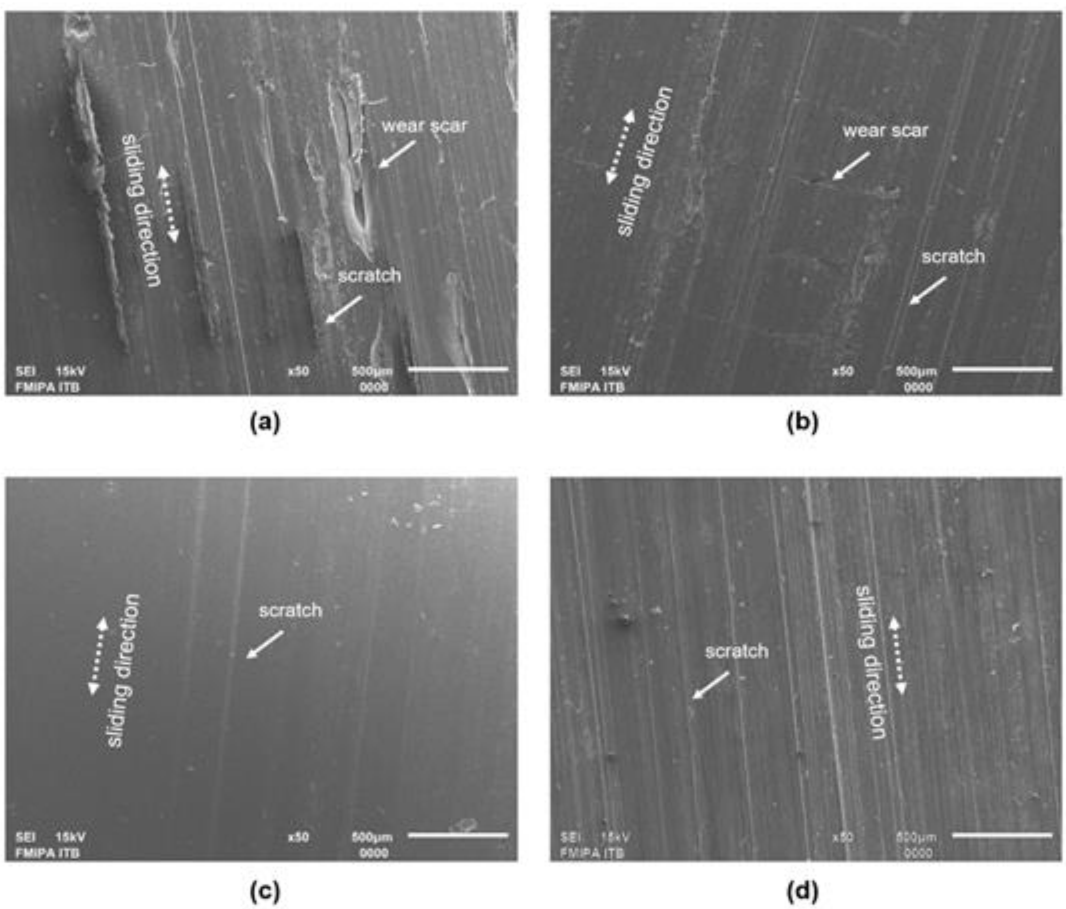

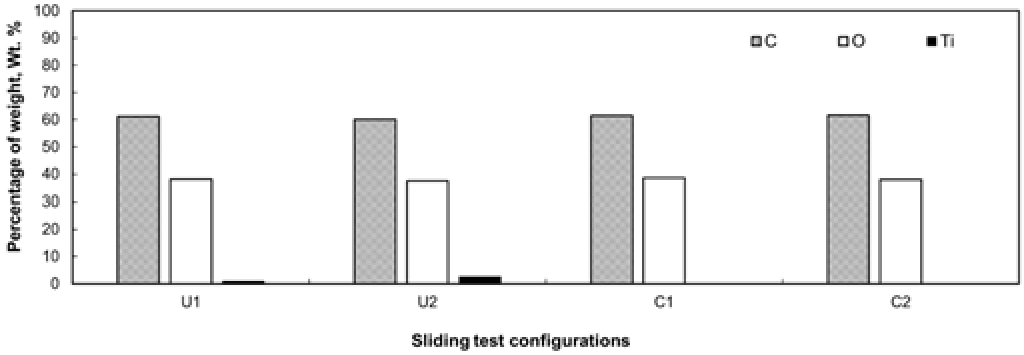

(e)

Figure 6. The worn surface morphologies of PLA pin after sliding up to 4×10^3 m for each sliding test configurations: (a) U1, (b) U2, (c) C1, (d) C2; and (e) the weight percentage of surface elemental compositions, as a result of analysis by using EDS. The sliding direction of the PLA pin against the Ti plate is indicated by the white arrow in the micrographs.

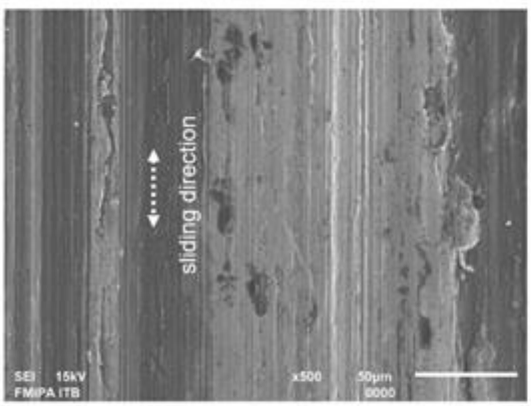

(a)

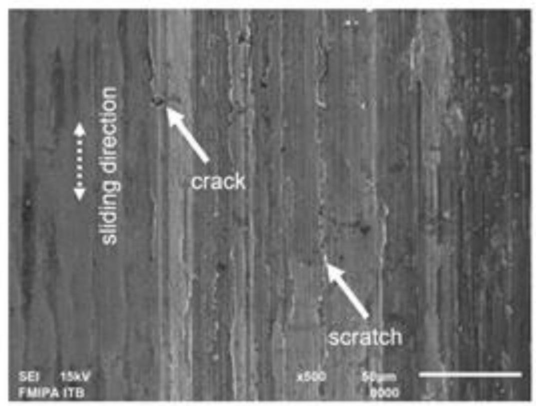

(b)

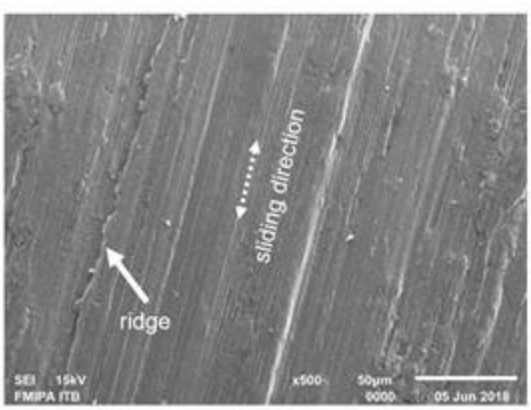

(c)

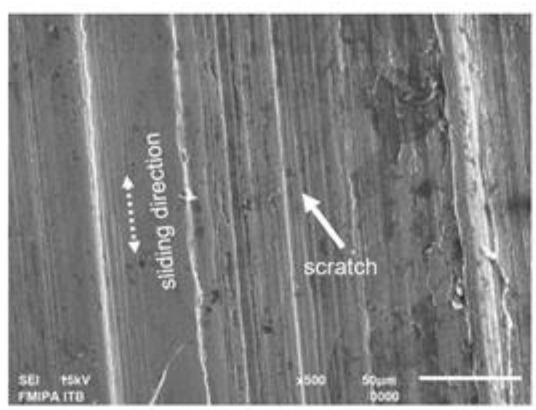

(d)

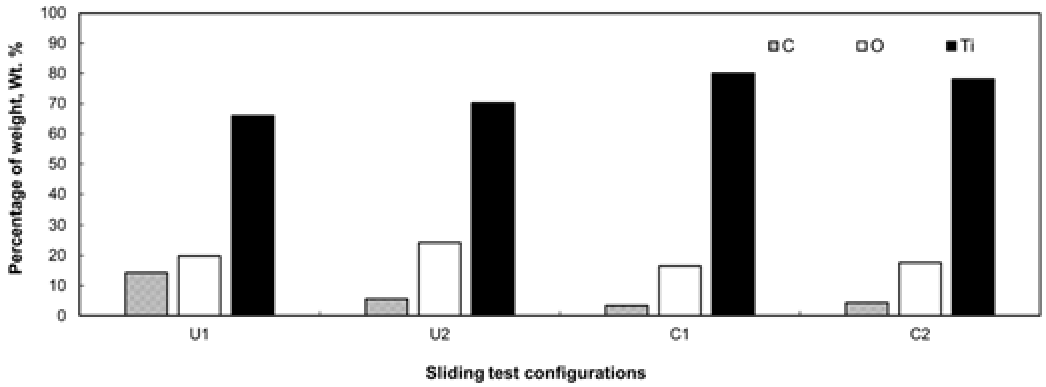

(e)

Figure 7. The worn surface morphologies of Ti plate after sliding up to 4×10^3 m for each sliding test configurations: (a) U1, (b) U2, (c) C1, (d) C2; and (e) the weight percentage of surface elemental compositions, as a result of analysis by using EDS. The sliding direction of the PLA pin against the Ti plate is indicated by the white arrow in the micrographs.

The worn surface of the Ti plate also indicated ploughing grooves and delaminated layer of this material, such as seen in Figures 7(a) – (d). During the sliding test, the Ti surface was ploughed, either by the sharp, hardened asperities of the PLA pin surface or its wear debris that were trapped at the interface of the pin and plate materials. Similar to the finding in a previous work [16], crack could also be seen on the ridges that were formed at the worn surface of Ti plate, as indicated in Figure. 7(b). The presence of cracks might demonstrate fatigue wear type that occurred over the surface of the Ti plate [16]. In addition to all these wear types, polymer film transfer mechanism might also occur during the sliding test, as indicated from the result of EDS analysis in Figure 7(e) where the presence of carbon trace element could be seen over the Ti surface. A similar finding of the polymer film transfer phenomenon could be seen in the work of Guezmil et al. [17]. As also reported earlier, polymer film transfers also caused roughening of the countersurface material [18, 19]. In this research, surface roughening of the Ti plate was evident, as indicated from the increasing R_a values of Ti surface in Table 2, which supported the possibility of wear mechanism by polymer film transfer operating alongside with abrasion that occurred during the sliding of FDM-processed PLA pin over the surface of Ti plate.

CONCLUSIONS

The influence of raster orientations on the wear resistance of FDM-processed polylactic-acid (PLA) materials in bovine blood serum was investigated. Based on the results obtained, it is concluded that the raster orientation applied in FDM determined the wear resistance of the printed PLA material once sliding over the surface of Ti plate. In this case, the PLA pins printed with crossed raster orientation were more resistant to wear than those printed with unidirectional raster orientation, as indicated by the lower *WF* value of the former pins, i.e., $\sim 0.9 \times 10^{-4}$ mm N^{-1} m^{-1} than that of the later ones, i.e., $\sim 1.5 \times 10^{-4}$ mm N^{-1} m^{-1}. Meanwhile, the *WF* value of Ti surface that slid against PLA pin with crossed raster orientation, i.e., ~0.09×10^{-4} mm N^{-1} m^{-1}, was also significantly lower than those sliding with the pin having unidirectional raster orientation, i.e., $0.34 – 0.41 \times 10^{-4}$ mm N^{-1} m^{-1}. Surface abrasion, fatigue and polymer film transfer were apparently the possible wear mechanisms of both the FDM-processed PLA pin and its Ti countersurface material during the sliding test.

REFERENCES

[1] Ventola CL. Medical applications for 3D printing: Current and projected uses. Pharmacy and Therapeutics. 2014; 39: 704-711.

[2] Mertz L. Dream it, design it, print it in 3-D. IEEE Pulse, 2013; 4(6): 15-21.

[3] Bogue R. 3D printing: The dawn of a new era in manufacturing? Assembly Automation. 2013; 33(4): 307-311.

[4] Espalin D, Arcaute K, Rodriguez D, Medina F. Fused deposition modelling of patient-specific polymethylmethacrylate implants. Rapid Prototyping Journal. 2010; 16(3): 164-173.

[5] Thomas DJ. 3D printing durable patient specific knee implants. Journal of Orthopaedics. 2017;14(1):182-183.

[6] Li Z, Liu H. What we have achieved in the design of 3D printed metal implants for application in orthopaedics? Personal experience and review. Rapid Prototyping Journal. 2018; 24(8): 1365-1379.

[7] Mohamed, OA, Masood, SH, Bhowmik, JL. Optimization of fused deposition modeling process parameters: A review of current research and future prospects, Advanced Manufacturing. 2015; 3:42–53.

[8] Sood AK, Equbal A, Toppo V, Ohdar RK, Mahapatra SS. An investigation on sliding wear of FDM built parts. CIRP Journal of Manufacturing Science and Technology. 2012; 5(1): 48-54.

[9] Equbal A, Sood AK, Toppo V, Ohdar RK, Mahapatra SS. Prediction and analysis of sliding wear performance of fused deposition modelling-processed ABS plastic parts. Proceedings of the Institution of Mechanical Engineers, Part J: Journal of Engineering Tribology. 2010; 224: 1261-1271.

[10] Mohamed OH, Masood SH, Bhowmik JL. Analysis of wear behavior of additively manufactured PC-ABS parts. Materials Letters. 2018; 230: 261-265.

[11] Borges RA, Choudury D, Zou M. 3D printed PCU/UHMWPE polymeric blend for artificial knee meniscus. Tribology International. 2018; 122: 1-7.

[12] Zdero R, Guenther LE, Gascoyne TC. Pin-on-disc wear testing of biomaterials used for total joint replacements. In: Zdero R, editor. Experimental Methods in Orthopaedic Biomechanics, London: Academic Press, 2017, p 299-311.

[13] Brown SS, Clarke IC. A review of lubrication conditions for wear simulation in artificial hip replacement. Tribology Transactions. 2006; 49: 72-78.

[14] Prayoga BT, Suyitno S, Dharmastiti R. The wear behavior of UHMWPE against surface modified cp-titanium by thermal oxidation. Tribology in Industry. 2016; 38(4): 543-551.

[15] Rajpurohit SR, Dave HK. Effect of process parameters on tensile strength of FDM printed PLA part. Rapid Prototyping Journal. 2018; 24(8): 1317-1324.
[16] Attar H, Prashanth KG, Chaubey AK, Calin M, Zhang LC, Scudino S, Eckert J. Comparison of wear properties of commercially pure titanium prepared by selective laser melting and casting processes. Materials Letters. 2015; 142: 38-41.
[17] Guezmil M, Bensalah W, Mezlini S. Tribological behavior of UHMWPE against $TiAl_6V_4$ and $CoCr_{28}Mo$ alloys under dry and lubricated conditions. Journal the Mechanical Behavior of Biomedical Materials. 2016; 63: 375-385.
[18] Cooper JR, Dowson D, Fisher J. The effect of transfer film and surface roughness on the wear of lubricated ultra-high molecular weight polyethylene. Clinical Materials. 1993; 14: 295-302.
[19] Bahadur S. The development of transfer layers and their role in polymer tribology. Wear. 2000; 245(1-2) 92-99.